

| | |
|---|-----|
| Reflection, Transmission, and Phase Shift | 422 |
| Index of Refraction | 425 |
| Dispersion Equations | 427 |
| CVI Standard Size Codes and Radii of Curvature | 428 |
| Radii Tolerance Chart | 429 |
| Optical Specifications | 430 |
| Optical Materials | 431 |
| Antireflection Coating | 438 |
| Waveplate Optical Axis Markings . . | 442 |
| Index | 443 |
| Product Code Index | 446 |
| Working with CVI | 448 |

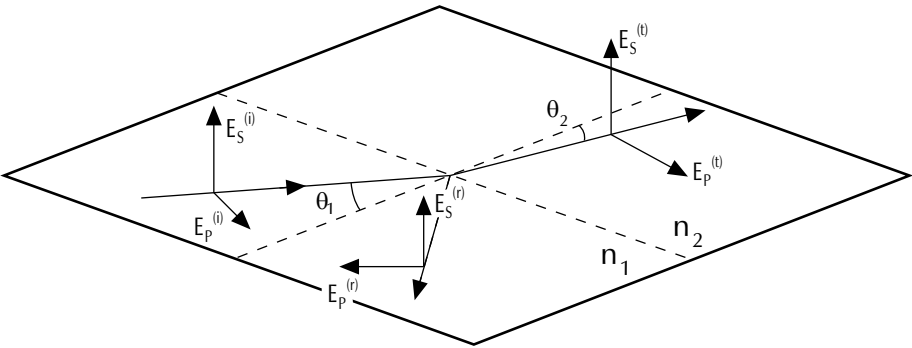
Reflection and Transmission Behavior at a Dielectric Interface

1. Fresnel's Equations

Fresnel's equations relate the amplitudes for reflection and transmission to the incident field amplitude at a dielectric interface. From these equations, the power reflectivity and transmissivity can be calculated, as well as the phase

shifts for reflected and transmitted wave. Below, we assume that all optical properties in the two media are governed by real indices of refraction and neglect inhomogeneities at the surface and in the bulk, thus ignoring scattering losses. The

form of Fresnel's equations depends in detail on the initial choice of positive field components, which are defined in the diagram below.



The plane of incidence and positive field component definitions in Fresnel's equations. The plane of incidence contains the normal to the interface and the propagation vectors of the incident, reflected, and transmitted waves. The electric field perpendicular to the plane of incidence is called the S polarized component. The electric field parallel to the plane of incidence is called the P polarized component.

Fresnel's Equations in the Absence of Total Internal Reflection

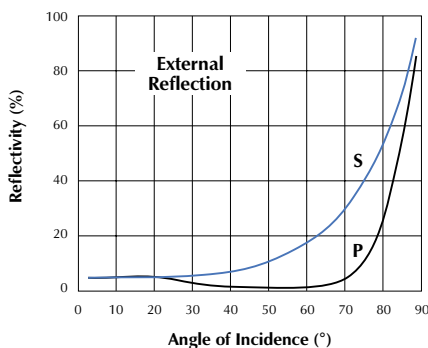
| Symbol | Description | Equation |
|--------|----------------------------------|---|
| t_p | P polarized Field Transmittivity | $t_p = \frac{E_P^{(t)}}{E_P^{(i)}} = \frac{2n_1 \cos\theta_1}{n_2 \cos\theta_1 + n_1 \cos\theta_2}$ |
| t_s | S polarized Field Transmittivity | $t_s = \frac{E_S^{(t)}}{E_S^{(i)}} = \frac{2n_1 \cos\theta_1}{n_1 \cos\theta_1 + n_2 \cos\theta_2}$ |
| r_p | P polarized Field Reflectivity | $r_p = \frac{E_P^{(r)}}{E_P^{(i)}} = \frac{n_2 \cos\theta_1 - n_1 \cos\theta_2}{n_2 \cos\theta_1 + n_1 \cos\theta_2}$ |
| r_s | S polarized Field Reflectivity | $r_s = \frac{E_S^{(r)}}{E_S^{(i)}} = \frac{n_1 \cos\theta_1 - n_2 \cos\theta_2}{n_1 \cos\theta_1 + n_2 \cos\theta_2}$ |
| R_p | P polarized Power Reflectivity | $R_p = \frac{\tan^2 (\theta_1 - \theta_2)}{\tan^2 (\theta_1 + \theta_2)}$ |
| R_s | S polarized Power Reflectivity | $R_s = \frac{\sin^2 (\theta_1 - \theta_2)}{\sin^2 (\theta_1 + \theta_2)}$ |

continued

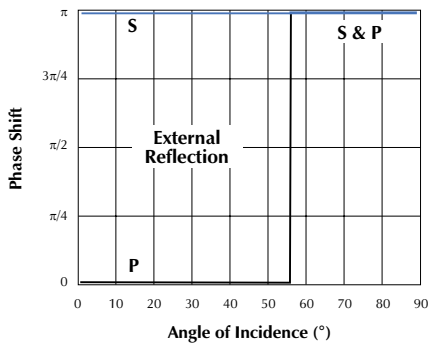
In Fresnel's Equations, θ_2 is calculated from Snell's Law:

$$n_1 \sin \theta_1 = n_2 \sin \theta_2.$$

The equations in the table are valid whenever θ_2 is a real angle. This is always true for external reflection, where $n_1 < n_2$, and is true for θ_1 less than the critical angle in internal reflection, where $n_1 > n_2$, discussed below. Plotted below are the power reflectivities and phase shifts for the S and P components. The



Power reflectivity at an $n = 1$ to $n = 1.50$ air-glass interface. Light is incident in air (external reflection).



Phase shift upon reflection at an $n = 1$ to $n = 1.50$ interface. Light is incident in air (external reflection). Transmitted phase shift is zero for both components.

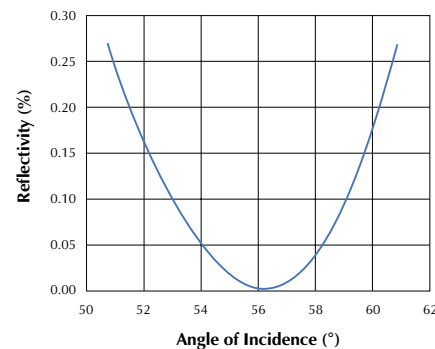
apparent phase shift disagreement at normal incidence is resolved by referring to the original definition of positive field components in the figure at the beginning of this section.

2. Brewster's Angle

Referring to the plot in the previous section, as the angle of incidence is increased from 0° , the P polarized reflectivity decreases, reaching a minimum near 56° . This minimum gives zero reflectivity and is attained at Brewster's angle,

$$\theta_B = \tan^{-1} (n_2 / n_1)$$

This phenomenon affords the laser designer a loss-free surface for the P component - something that was realized early in the history of laser research. A question often arises: How far from Brewster's angle can the beam be, and still have relatively low loss for P polarization? This is answered in the plot below.



P polarized reflectivity at an $n = 1$ to $n = 1.50$ air-glass interface near Brewster's angle. Light is incident in air (external reflection).

The region where the P component reflectivity is less than 0.25% is approximately $\pm 4^\circ$ to either side of Brewster's angle.

3. Internal Reflection and the Critical Angle

The term internal reflection is used when $n_1 > n_2$ (ie. when light is incident in the material of higher index of refraction). Internal reflection can be partial or total

depending on whether the incidence angle exceeds the critical angle. Referring to Snell's Law, when $n_1 > n_2$, it is possible to choose an incidence angle θ_1 for which a real value of the angle of refraction θ_2 does not exist. This will occur for angles of incidence $\theta_1 > \theta_C$ where θ_C is the critical angle,

$$\theta_C = \sin^{-1} (n_2 / n_1), \text{ for } n_2 < n_1$$

For light at an angle of incidence less than the critical angle, the equations in the table in Sec. 1 can be used without alteration, taking care to insert the higher index of refraction for n_1 .

Above the critical angle, total internal reflection occurs. Far from the interface, for $\theta_1 > \theta_C$, $n_2 < n_1$:

$$r_P = \frac{(n_2/n_1)^2 \cos \theta_1 - i \sqrt{\sin^2 \theta_1 - (n_2/n_1)^2}}{(n_2/n_1)^2 \cos \theta_1 + i \sqrt{\sin^2 \theta_1 - (n_2/n_1)^2}}$$

$$r_S = \frac{\cos \theta_1 - i \sqrt{\sin^2 \theta_1 - (n_2/n_1)^2}}{\cos \theta_1 + i \sqrt{\sin^2 \theta_1 - (n_2/n_1)^2}}$$

$$t_P = t_S = 0$$

Above the critical angle, the field reflectivities have modulus 1; they are in the form of pure phase shifts. The power reflectivity is 100%. The P and S phase shifts differ and are functions of the angle of incidence and the relative index $n = n_2 / n_1$. The formula for the relative phase shift is:

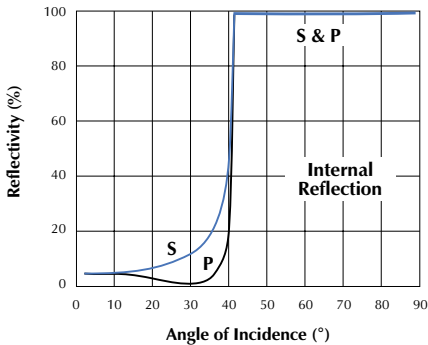
$$\delta = \phi_s - \phi_p = 2 \tan^{-1} \left[\frac{\cos \theta_1 \sqrt{\sin^2 \theta_1 - n^2}}{\sin^2 \theta_1} \right]$$

continued

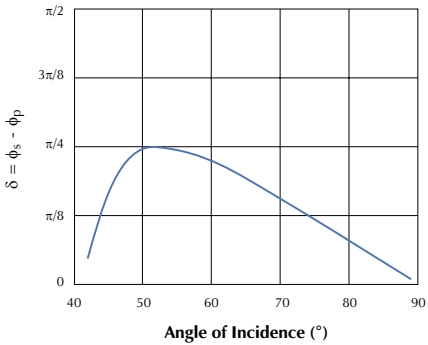
Reflection, Transmission, & Phase Shift

Technical Notes

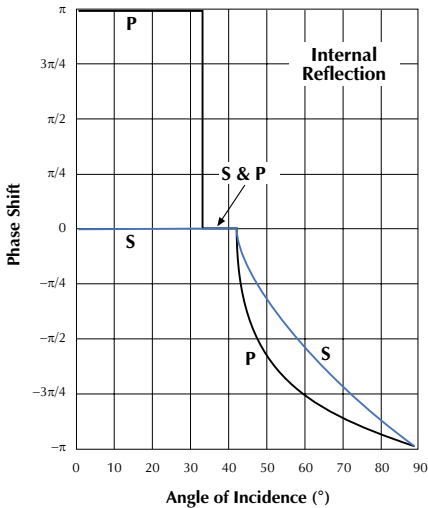
Plots for the power reflectivity, absolute phase shifts, and relative S to P phase shifts are shown.



Power reflectivity at an $n = 1.5$ to $n = 1$ glass-air interface. Light is incident in glass (internal reflection). The critical angle is approximately 41.8° .



Relative phase shift $\phi_S - \phi_P$ for $n = 1.5$ to $n = 1$ total internal reflection.



Reflected phase shifts at an $n = 1.5$ to $n = 1$ glass-air interface. Light is incident in glass (internal reflection).

The relative phase shift $\phi_S - \phi_P$ leads to an elliptically polarized reflected beam unless the incident beam is pure S or P polarization. This effect is utilized to create circularly polarized light in a Fresnel Rhomb Retarder and should be kept in mind when using right angle prisms to route beams in the lab.

Ultraviolet Materials

| Wavelength (nm) | MgF ₂ | | CaF ₂ | Sapphire | | Crystal Quartz | | Fused Silica |
|--------------------|------------------|----------------|------------------|----------------|----------------|----------------|----------------|--------------|
| | n _e | n _o | n | n _e | n _o | n _e | n _o | |
| 193 | 1.44127 | 1.42767 | 1.50153 | 1.91743 | 1.92879 | 1.67455 | 1.66091 | 1.56077 |
| 213 | 1.42933 | 1.41606 | 1.48544 | 1.87839 | 1.88903 | 1.64452 | 1.63224 | 1.53539 |
| 222 | 1.42522 | 1.41208 | 1.47996 | 1.86504 | 1.87540 | 1.63427 | 1.62238 | 1.52669 |
| 226 | 1.42358 | 1.41049 | 1.47779 | 1.85991 | 1.87017 | 1.63033 | 1.61859 | 1.52335 |
| 244 | 1.41735 | 1.40447 | 1.46957 | 1.84075 | 1.85059 | 1.61562 | 1.60439 | 1.51086 |
| 248 | 1.41618 | 1.40334 | 1.46803 | 1.83719 | 1.84696 | 1.61289 | 1.60175 | 1.50855 |
| 257 | 1.41377 | 1.40102 | 1.46488 | 1.82972 | 1.83932 | 1.60714 | 1.59620 | 1.50368 |
| 266 | 1.41164 | 1.39896 | 1.46209 | 1.82358 | 1.83304 | 1.60242 | 1.59164 | 1.49968 |
| 280 | 1.40877 | 1.39620 | 1.45836 | 1.81509 | 1.82437 | 1.59589 | 1.58533 | 1.49416 |
| 308 | 1.40429 | 1.39188 | 1.45255 | 1.80198 | 1.81096 | 1.58577 | 1.57556 | 1.48564 |
| 325 | 1.40216 | 1.38983 | 1.44981 | 1.79582 | 1.80467 | 1.58102 | 1.57097 | 1.48164 |
| 337 | 1.40086 | 1.38859 | 1.44814 | 1.79206 | 1.80082 | 1.57812 | 1.56817 | 1.47919 |
| 351 | 1.39952 | 1.38730 | 1.44642 | 1.78825 | 1.79693 | 1.57518 | 1.56533 | 1.47672 |
| 355 | 1.39917 | 1.38696 | 1.44597 | 1.78732 | 1.79598 | 1.57446 | 1.56463 | 1.47612 |

Visible Materials

| Wavelength (nm) | Schott BK7 | Schott F2 | Schott SF10 | Schott SF11 | Schott N-LaF34 | Crystal Quartz | | Fused Silica |
|--------------------|---------------|--------------|----------------|----------------|-------------------|----------------|----------------|--------------|
| | | | | | | n _e | n _o | |
| 400 | 1.53085 | 1.65215 | 1.77826 | 1.84512 | 1.80039 | 1.56730 | 1.55772 | 1.47012 |
| 442 | 1.52611 | 1.64058 | 1.75970 | 1.82242 | 1.79073 | 1.56266 | 1.55324 | 1.46622 |
| 458 | 1.52461 | 1.63716 | 1.75434 | 1.81592 | 1.78780 | 1.56119 | 1.55181 | 1.46498 |
| 488 | 1.52224 | 1.63178 | 1.74602 | 1.80590 | 1.78310 | 1.55885 | 1.54955 | 1.46301 |
| 515 | 1.52049 | 1.62784 | 1.73999 | 1.79867 | 1.77960 | 1.55711 | 1.54787 | 1.46156 |
| 532 | 1.51947 | 1.62569 | 1.73673 | 1.79479 | 1.77767 | 1.55610 | 1.54690 | 1.46071 |
| 590 | 1.51670 | 1.61983 | 1.72794 | 1.78435 | 1.77231 | 1.55333 | 1.54421 | 1.45838 |
| 633 | 1.51509 | 1.61654 | 1.72307 | 1.77860 | 1.76923 | 1.55171 | 1.54264 | 1.45702 |
| 670 | 1.51391 | 1.61421 | 1.71965 | 1.77458 | 1.76702 | 1.55051 | 1.54148 | 1.45601 |
| 694 | 1.51322 | 1.6129 | 1.71773 | 1.77233 | 1.76576 | 1.54981 | 1.54080 | 1.45542 |
| 755 | 1.51172 | 1.61009 | 1.71367 | 1.76758 | 1.76302 | 1.54827 | 1.53932 | 1.45414 |
| 780 | 1.51118 | 1.60911 | 1.71227 | 1.76595 | 1.76205 | 1.54771 | 1.53878 | 1.45367 |
| 800 | 1.51078 | 1.60839 | 1.71124 | 1.76475 | 1.76132 | 1.54729 | 1.53837 | 1.45332 |
| 820 | 1.51039 | 1.60771 | 1.71028 | 1.76364 | 1.76064 | 1.54688 | 1.53798 | 1.45298 |
| 860 | 1.50966 | 1.60648 | 1.70854 | 1.76163 | 1.75938 | 1.54612 | 1.53724 | 1.45234 |
| 980 | 1.50779 | 1.60349 | 1.70441 | 1.75688 | 1.75623 | 1.54409 | 1.53531 | 1.45067 |
| 1064 | 1.50663 | 1.60183 | 1.70217 | 1.75434 | 1.75439 | 1.54282 | 1.53410 | 1.44963 |
| 1320 | 1.50346 | 1.59785 | 1.69706 | 1.74863 | 1.74965 | 1.53922 | 1.53068 | 1.44669 |
| 1550 | 1.50065 | 1.59487 | 1.69348 | 1.74474 | 1.74576 | 1.53596 | 1.52761 | 1.44402 |
| 2010 | 1.49435 | 1.58905 | 1.68693 | 1.73784 | 1.73747 | 1.52863 | 1.52073 | 1.43794 |

For up-to-date information on materials compliance with the European Union RoHS ► www.cvilaser.com

Infrared Materials

| Wavelength (μm) | Zinc Selenide ZnSe | IR grade Calcium Fluoride CFIR | Germanium Ge | Silicon Si |
|--------------------|-----------------------|-----------------------------------|-----------------|---------------|
| 0.6328 | 2.590 | 1.43289 | 5.3900 | 3.9200 |
| 1.40 | 2.461 | 1.42673 | 4.3400 | 3.4900 |
| 1.50 | 2.458 | 1.42626 | 4.3500 | 3.4800 |
| 1.66 | 2.454 | 1.42551 | 4.3300 | 3.4700 |
| 1.82 | 2.449 | 1.42475 | 4.2900 | 3.4600 |
| 2.05 | 2.446 | 1.42360 | 4.2500 | 3.4500 |
| 2.06 | 2.446 | 1.42355 | 4.2400 | 3.4900 |
| 2.15 | 2.444 | 1.42308 | 4.2400 | 3.4700 |
| 2.44 | 2.442 | 1.42146 | 4.0700 | 3.4700 |
| 2.50 | 2.441 | 1.42110 | 4.2200 | 3.4400 |
| 2.58 | 2.440 | 1.42062 | 4.0600 | 3.4364 |
| 2.75 | 2.439 | 1.41954 | 4.0526 | 3.4335 |
| 3.00 | 2.438 | 1.41785 | 4.0540 | 3.4307 |
| 3.42 | 2.436 | 1.41469 | 4.0370 | 3.4277 |
| 3.50 | 2.435 | 1.41404 | 4.0356 | 3.4272 |
| 4.36 | 2.432 | 1.40609 | 4.0227 | 3.4223 |
| 5.00 | 2.430 | 1.39896 | 4.0177 | 3.4203 |
| 6.00 | 2.426 | 1.38560 | 4.0138 | 3.4188 |
| 6.24 | 2.425 | 1.38197 | 4.0100 | 3.4185 |
| 7.50 | 2.420 | 1.36000 | 4.0095 | 3.4171 |
| 8.66 | 2.414 | 1.33504 | 4.0071 | 3.4161 |
| 9.50 | 2.410 | 1.31375 | 4.0064 | 3.4158 |
| 9.72 | 2.409 | 1.30768 | 4.0062 | 3.4155 |
| 10.60 | 2.400 | 1.28116 | 4.0058 | 3.4155 |
| 11.00 | 2.400 | 1.26783 | 4.0059 | 3.4155 |
| 11.04 | 2.400 | 1.26645 | 4.0059 | 3.4155 |
| 12.50 | 2.390 | 1.20951 | 4.0000 | 3.4155 |
| 13.02 | 2.385 | 1.18573 | 4.0000 | 3.4155 |
| 13.50 | 2.380 | 1.16187 | 4.0000 | 3.4155 |
| 15.00 | 2.370 | 1.07290 | 4.0000 | 3.4155 |
| 16.00 | 2.360 | 0.99783 | 4.0000 | 3.4155 |
| 16.90 | 2.350 | 0.91507 | 4.0000 | 3.4155 |
| 17.80 | 2.340 | 0.81173 | 4.0000 | 3.4155 |
| 18.60 | 2.330 | 0.69336 | 4.0000 | 3.4155 |
| 19.30 | 2.320 | 0.55456 | 4.0000 | 3.4155 |
| 20.00 | 2.310 | 0.34029 | 4.0000 | 3.4155 |

Note: Refractive index calculated at 25° C except for those from H.W. Icenogle reference which was calculated at 22.85° C.

Germanium 633-2500nm
Reference: S. Adachi, "Model dielectric constants of Si and Ge," *Phys. Rev. B*, Vol. 38, No. 18, 15 Dec. 1988, pp. 12966-12976.

Germanium 2750-11040nm
Reference: H. W. Icenogle, B. C. Platt, and W. L. Wolfe, "Refractive indexes and temperature coefficients of germanium and silicon," *Appl. Opt.* Vol. 15, No. 10, October 1976, pp. 2348-2351.

Germanium 12500-20000nm
Reference: G. Ghosh and H. Yajima, "Coefficients of a dispersion equation for the pressure-optic coefficients in Ge and GaAs," *Phys. Rev. B*, Vol. 59, No. 19, 15 May 1999, pp. 12208-12211.

ZnSe
Values from 446 to 700 nm are from Ref. 1. Index values for wavelengths beyond 700 nm are from Ref. 2 and apply to bulk ZnSe.

References:
[1] M. Ukita, H. Okuyama, M. Ozawa, A. Ishibashi, K. Akimoto, and Y. Mori, "Refractive index of ZnMgSSe alloys lattice matched to GaAs," *Appl. Phys. Lett.*, Vol. 63, No. 15, 11 October 1993, pp. 2082-2084
[2] II-VI Incorporated Optics Catalog, July 1998 Revision, p. 6 and at www.ii-vi.com.

Si 633-2440nm
[1] S. Adachi, "Model dielectric constants of Si and Ge," *Phys.*

Rev. B, Vol. 38, No. 18, 15 Dec. 1988, pp. 12966-12976.

[2] J. Humlíček, M. Garriga, M. I. Alonso, and M. Cardona, "Optical spectra of SixGe1-x alloys," *J. Appl. Phys.* Vol. 65, No. 7, 1 April 1989, pp. 2827-2832.

Si 2580-9720nm
Reference: H. W. Icenogle, B. C. Platt, and W. L. Wolfe, "Refractive indexes and temperature coefficients of germanium and silicon," *Appl. Opt.* Vol. 15, No. 10, October 1976, pp. 2348-2351.

Si 10600nm
[1] J. Lamb, Miscellaneous data on materials for millimetre and submillimetre optics, www.ovro.caltech.edu/~lamb/ALMA/Receivers/mmMaterialProperties1.pdf

Dispersion Equations for Optical Materials

We use a Sellmeier equation to describe the dispersion of common materials, except crystal quartz. The equation used is:

$$n^2 = 1 + \frac{B_1 \lambda^2}{\lambda^2 - C_1} + \frac{B_2 \lambda^2}{\lambda^2 - C_2} + \frac{B_3 \lambda^2}{\lambda^2 - C_3}$$

where the wavelength, λ , is expressed in μm .

For crystal quartz, a "Laurent" series formula is used. It is:

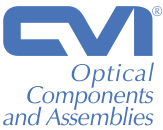
$$n^2 = B_1 + B_2 \lambda^2 + \frac{B_3}{\lambda^2} + \frac{C_1}{\lambda^4} + \frac{C_2}{\lambda^6} + \frac{C_3}{\lambda^8}$$

Below are the constants in the dispersion equation for various materials.

Dispersion Equation Constants

| | B ₁ | B ₂ | B ₃ | C ₁ | C ₂ | C ₃ |
|---------------------------------|----------------|-----------------|----------------|----------------|-----------------|----------------|
| Crystal Quartz n _e | 2.38490000E+00 | -1.25900000E-02 | 1.07900000E-02 | 1.65180000E-04 | -1.94741000E-06 | 9.36476000E-08 |
| Crystal Quartz n _o | 2.35728000E+00 | -1.17000000E-02 | 1.05400000E-02 | 1.34143000E-04 | -4.45368000E-07 | 5.92362000E-08 |
| MgF ₂ n _e | 4.13440230E-01 | 5.04974990E-01 | 2.49048620E+00 | 1.35737865E-03 | 8.23767167E-03 | 5.65107755E+02 |
| MgF ₂ n _o | 4.87551080E-01 | 3.98750310E-01 | 2.31203530E+00 | 1.88217800E-03 | 8.95188847E-03 | 5.66135591E+02 |
| Sapphire n _e | 1.50397590E+00 | 5.50691410E-01 | 6.59273790E+00 | 5.48041129E-03 | 1.47994281E-02 | 4.02895140E+02 |
| Sapphire n _o | 1.43134930E+00 | 6.50547130E-01 | 5.34140210E+00 | 5.27992610E-03 | 1.42382647E-02 | 3.25017834E+02 |
| CaF ₂ | 5.67588800E-01 | 4.71091400E-01 | 3.84847230E+00 | 2.52642999E-03 | 1.00783328E-02 | 1.20055597E+03 |
| Fused Silica | 6.96166300E-01 | 4.07942600E-01 | 8.97479400E-01 | 4.67914826E-03 | 1.35120631E-02 | 9.79340025E+01 |
| Schott BK7 | 1.03961212E+00 | 2.31792344E-01 | 1.01046945E+00 | 6.00069867E-03 | 2.00179144E-02 | 1.03560653E+02 |
| Schott N-BK7 | 1.03961212E+00 | 2.31792344E-01 | 1.01046945E+00 | 6.00069867E-03 | 2.00179144E-02 | 1.03560653E+02 |
| Schott F2 | 1.34533359E+00 | 2.09073118E-01 | 9.37357162E-01 | 9.97743871E-03 | 4.70450767E-02 | 1.11886764E+02 |
| Schott N-F2 | 1.39757037E+00 | 1.59201403E-01 | 1.26865430E+00 | 9.95906143E-03 | 5.46931752E-02 | 1.19248346E+02 |
| Schott SF2 | 1.40301821E+00 | 2.09073176E-01 | 9.39056586E-01 | 1.05795466E-02 | 4.93226978E-02 | 1.12405955E+02 |
| Schott SF10 | 1.61625977E+00 | 2.59229334E-01 | 1.07762317E+00 | 1.27534559E-02 | 5.81983954E-02 | 1.16607680E+02 |
| Schott N-SF10 | 1.62153902E+00 | 2.56287842E-01 | 1.64447552E+00 | 1.22241457E-02 | 5.95736775E-02 | 1.47468793E+02 |
| Schott SF11 | 1.73848403E+00 | 3.11168974E-01 | 1.17490871E+00 | 1.36068604E-02 | 6.15960463E-02 | 1.21922711E+02 |
| Schott N-SF11 | 1.73759695E+00 | 3.13747346E-01 | 1.89878101E+00 | 1.13188707E-02 | 6.23068142E-02 | 1.5523629E+02 |
| Schott N-LaF34 | 1.75836958E+00 | 3.13537785E-01 | 1.18925231E+00 | 8.72810026E-03 | 2.93020832E-02 | 8.51780644E+01 |
| Schott N-LAK21 | 1.22718116E+00 | 4.20783743E-01 | 1.01284843E+00 | 6.02075682E-03 | 1.96862889E-02 | 8.84370099E+01 |

CVI Standard Size Codes & Radii of Curvature



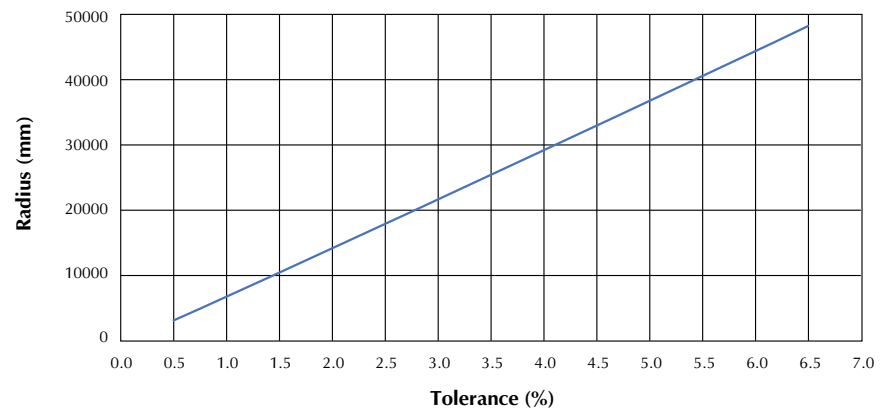
Technical Notes

| Size Code | 0537 | 0643 | 0737 | 0924 | 1025 | 1037 | 1537 | 2037 |
|----------------|--------|--------|--------|--------|--------|--------|--------|--------|
| Diameter | 0.500" | 15.0mm | 0.750" | 25.0mm | 1.000" | 1.000" | 1.500" | 2.000" |
| Thickness | 0.375" | 11.0mm | 0.375" | 6.0mm | 0.250" | 0.375" | 0.375" | 0.375" |
| Concave Radius | | | | | | | | |
| 0.010m | ● | ○ | ○ | ○ | ○ | ● | na | na |
| 0.025m | ● | ○ | ● | ● | ● | ● | ○ | na |
| 0.050m | ● | ○ | ● | ● | ● | ● | ○ | ○ |
| 0.060m | ○ | ○ | ○ | ○ | ○ | ● | ○ | ○ |
| 0.075m | ● | ○ | ○ | ● | ● | ● | ○ | ○ |
| 0.10m | ● | ● | ● | ● | ● | ● | ○ | ○ |
| 0.15m | ● | ○ | ○ | ○ | ○ | ● | ○ | ○ |
| 0.20m | ● | ○ | ● | ○ | ○ | ● | ○ | ● |
| 0.25m | ● | ● | ● | ● | ● | ● | ● | ● |
| 0.30m | ● | ● | ● | ● | ● | ● | ○ | ● |
| 0.35m | ○ | ○ | ○ | ○ | ○ | ● | ○ | ○ |
| 0.40m | ○ | ○ | ○ | ○ | ○ | ● | ○ | ● |
| 0.45m | ○ | ○ | ○ | ○ | ○ | ● | ○ | ○ |
| 0.50m | ● | ● | ● | ● | ● | ● | ● | ● |
| 0.60m | ○ | ● | ○ | ○ | ○ | ● | ○ | ● |
| 0.75m | ● | ○ | ● | ○ | ○ | ● | ○ | ● |
| 0.90m | ○ | ○ | ○ | ○ | ○ | ● | ○ | ○ |
| 1.00m | ● | ● | ● | ● | ● | ● | ● | ● |
| 1.20m | ○ | ● | ○ | ○ | ○ | ● | ○ | ○ |
| 1.50m | ● | ○ | ● | ● | ● | ● | ○ | ● |
| 2.00m | ● | ● | ● | ● | ● | ● | ● | ● |
| 3.00m | ● | ● | ● | ● | ● | ● | ● | ● |
| 4.00m | ● | ● | ● | ● | ○ | ● | ● | ● |
| 5.00m | ● | ● | ● | ● | ● | ● | ● | ● |
| 6.00m | ● | ● | ● | ● | ● | ● | ● | ● |
| 7.00m | ● | ○ | ● | ○ | ○ | ● | ○ | ● |
| 8.00m | ● | ● | ● | ○ | ○ | ● | ● | ● |
| 9.00m | ● | ○ | ● | ○ | ○ | ● | ● | ● |
| 10.0m | ● | ● | ● | ● | ● | ● | ● | ● |
| 15.0m | ● | ○ | ● | ○ | ○ | ● | ● | ● |
| 20.0m | ● | ● | ● | ○ | ○ | ● | ● | ● |
| 30.0m | ○ | ○ | ○ | ○ | ○ | ● | ○ | ○ |
| Convex Radius | | | | | | | | |
| 0.050m | ○ | ○ | ○ | ○ | ○ | ● | ○ | ○ |
| 0.10m | ● | ● | ● | ● | ○ | ● | ● | ○ |
| 0.15m | ● | ○ | ○ | ○ | ○ | ○ | ○ | ○ |
| 0.20m | ● | ○ | ○ | ○ | ○ | ● | ○ | ○ |
| 0.30m | ○ | ● | ● | ● | ○ | ● | ● | ● |
| 0.40m | ○ | ○ | ○ | ○ | ○ | ● | ○ | ○ |
| 0.50m | ● | ○ | ● | ● | ○ | ● | ● | ● |
| 0.60m | ○ | ○ | ○ | ○ | ○ | ○ | ○ | ○ |
| 0.75m | ○ | ● | ○ | ○ | ○ | ● | ○ | ● |
| 1.00m | ○ | ● | ● | ● | ○ | ● | ● | ● |
| 1.50m | ○ | ○ | ○ | ○ | ○ | ● | ○ | ● |
| 2.00m | ○ | ● | ● | ● | ○ | ● | ● | ● |
| 2.50m | ○ | ○ | ○ | ○ | ○ | ● | ○ | ○ |
| 3.00m | ○ | ○ | ● | ○ | ○ | ● | ○ | ● |
| 4.00m | ○ | ○ | ● | ○ | ○ | ● | ● | ● |
| 5.00m | ○ | ○ | ● | ● | ○ | ● | ● | ● |
| 6.00m | ○ | ○ | ○ | ○ | ○ | ● | ○ | ● |
| 7.00m | ○ | ○ | ○ | ○ | ○ | ● | ○ | ● |
| 8.00m | ○ | ○ | ○ | ○ | ○ | ● | ● | ● |
| 9.00m | ○ | ○ | ● | ○ | ○ | ● | ○ | ● |
| 10.0m | ○ | ○ | ○ | ○ | ○ | ● | ○ | ● |
| 15.0m | ○ | ○ | ○ | ○ | ○ | ● | ○ | ● |
| 20.0m | ○ | ○ | ○ | ○ | ○ | ● | ● | ● |

● Standard radius ○ Optional radius for Radii Tolerance Chart ▶ 429

CVI Radii Tolerance

| Tolerance % | Radius (mm) | How to read this chart |
|---|-------------|--|
| 0.5 | 3500 | If $R \leq 3500\text{mm}$ then Radius Tolerance is 0.5% |
| 1.0 | 7000 | If $3501\text{mm} \leq R \leq 7000\text{mm}$ then Radius Tolerance is 1% |
| 1.5 | 10500 | If $7501\text{mm} \leq R \leq 10500\text{mm}$ then Radius Tolerance is 1.5% |
| 2.0 | 14300 | If $10501\text{mm} \leq R \leq 14300\text{mm}$ then Radius Tolerance is 2.0% |
| 2.5 | 18000 | If $14301\text{mm} \leq R \leq 18000\text{mm}$ then Radius Tolerance is 2.5% |
| 3.0 | 21750 | If $18001\text{mm} \leq R \leq 21750\text{mm}$ then Radius Tolerance is 3.0% |
| 3.5 | 25500 | If $21751\text{mm} \leq R \leq 25500\text{mm}$ then Radius Tolerance is 3.5% |
| 4.0 | 29000 | If $25501\text{mm} \leq R \leq 29000\text{mm}$ then Radius Tolerance is 4.0% |
| 4.5 | 33000 | If $29001\text{mm} \leq R \leq 33000\text{mm}$ then Radius Tolerance is 4.5% |
| 5.0 | 37000 | If $33001\text{mm} \leq R \leq 37000\text{mm}$ then Radius Tolerance is 5.0% |
| 5.5 | 40000 | If $37001\text{mm} \leq R \leq 40000\text{mm}$ then Radius Tolerance is 5.5% |
| 6.0 | 44800 | If $40001\text{mm} \leq R \leq 44800\text{mm}$ then Radius Tolerance is 6.0% |
| 6.5 | 48800 | If $44801\text{mm} \leq R \leq 48800\text{mm}$ then Radius Tolerance is 6.5% |
| Greater than 48800mm will need special consideration. | | |



Radius of Curvature

For short radius lenses, spherical aberration is the major contributor of wavefront distortion. This transition happens at or about $f/10$. CVI uses this as a practical limit to optimize the manufacturing process. Further improvements to surface figure do not result in measurable improvements to the overall wavefront distortion and will only increase cost. Use the following charts as a guide for when spherical aberration dominates the wavefront distortion.

Practical Limits to Surface Figure for Short Radius Lenses

| Radius of Curvature if \leq | Diameter if \leq | Surface Figure |
|-------------------------------|--------------------|----------------|
| Spherical Lenses | | |
| 31.00mm | 12.70mm | $\lambda/4$ |
| 75.00mm | 25.40mm | $\lambda/4$ |
| 125.00mm | 38.10mm | $\lambda/4$ |
| 185.00mm | 50.80mm | $\lambda/4$ |
| 315.00mm | 76.20mm | $\lambda/4$ |
| Cylindrical Lenses | | |
| 31.00mm | 12.70mm | λ |
| 75.00mm | 15.00mm | λ |
| 125.00mm | 20.00mm | λ |
| 185.00mm | 25.40mm | λ |
| 315.00mm | 30.00mm | λ |

Substrate material

The material from which an optic is made.

The most common materials are BK7, UV grade fused silica, MgF_2 , and CaF_2 . CVI has experience with a wide variety of glasses, fused silicas, and crystalline materials. See the Optical Materials section ► **431-437**

Surface figure

The deviation from the ideal surface.

CVI specifies surface figure in terms of waves peak-to-valley at 633nm, prior to coating. The peak-to-valley specification is more stringent than an RMS or average surface specification and assures high quality parts for all applications. CVI can produce flats to $\lambda/20$ and spherical surfaces to $\lambda/10$ accuracy on a routine basis. A coated surface figure may also be specified; please contact CVI.

Cosmetic Surface Quality

Surface quality describes a level of defects visually detected on the surface of an optical component. CVI performs 100% visual inspection on all optics. Surface quality becomes critically important in high energy laser applications or where scatter must be reduced for better signal to noise performance.

MIL-PRF-13830B

This inspection criteria was adopted in 1997. The first number denotes the size and concentration of scratches as compared to a known NIST standard. The second number defines the largest pit by its diameter in hundredths of millimeters. For example: 10 dig = $\frac{1}{2}(\text{Length of dig} + \text{Width of dig}) = 0.1 \text{ mm diameter}$.

CVI Laser Quality

CVI has extensive experience in delivering high laser damage threshold optics and has developed a proprietary inspection method to consistently meet our customers' laser induced damage requirements. This proprietary inspection method utilizes significantly brighter light

sources than those specified in MIL-PRF-13830B. CVI also utilizes magnification when required to detect scratches, digs and other imperfections.

Laser Grade

Laser grade is the highest level of inspection criteria in the optics industry. Laser grade optics are virtually defect-free. High power magnification is used to detect and measure defects.

Wedge

The angle between the two surfaces of an optical element.

This can also be expressed as the difference in edge thickness around the part, for example a 25.4mm diameter optic with an edge thickness variation of 0.025mm has a wedge of 3.44 minutes of arc.

Radius of curvature

The radius of the sphere coincident with the optical surface.

A flat has radius of curvature equal to infinity. The reciprocal of the radius is called the curvature of the surface. CVI can manufacture a wide range of curvatures using its existing tooling and test plates and has the capability to make new test plates if required. CVI's standard radius tolerance is $\pm 0.5\%$ and $\pm 0.1\%$ is available for selected radii.

Concentricity

The deviation between the optical and mechanical axes of a lens.

Concentricity error is the measured maximum edge thickness variation. CVI's standard concentricity is $\leq 0.05\text{mm}$ edge thickness variation.

Clear aperture

The central area over which the optical specifications apply.

CVI specifies clear aperture in terms of the diameter or linear dimensions of this central area.

Angle and plane of incidence

The angle formed between the normal to the optical surface and the incident ray.

An incidence angle of zero degrees is referred to as normal incidence. The plane of incidence is the plane containing the incident ray and the normal.

Polarization

The orientation and phase shift of the electric field when resolved into components parallel and perpendicular to the plane of incidence.

P polarized light has the electric field polarized parallel to the plane of incidence. S polarized light has the electric field polarized perpendicular to the plane of incidence. UNP refers to unpolarized light, which is a random mixture of equal amounts of S and P polarization states. Specify the polarization state whenever ordering an optic for use at non-normal incidence angle.

Damage threshold

Damage threshold is typically higher for antireflection coatings than for high reflector coatings due to the nature of the coating materials.

Typical Damage Threshold Data

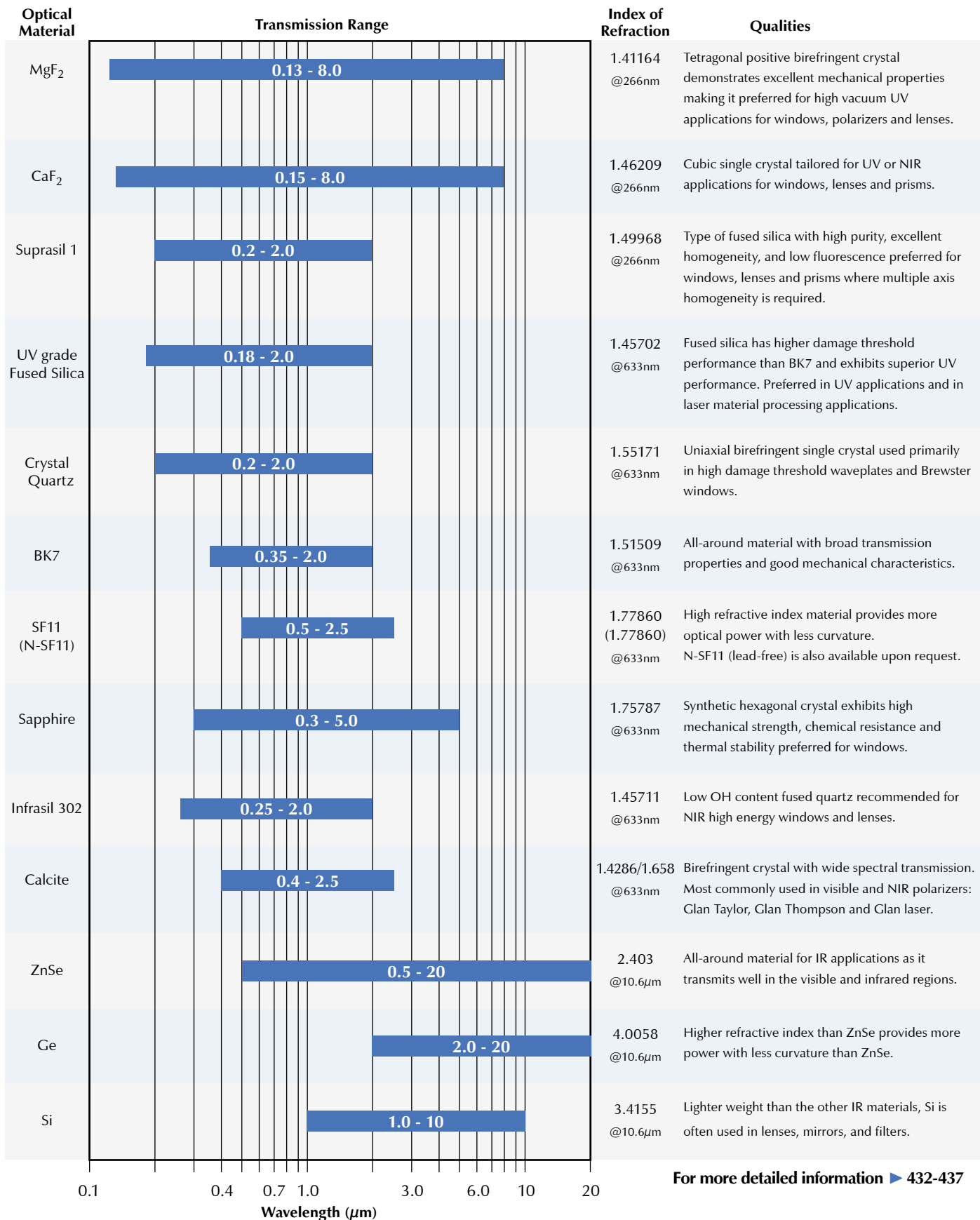
UV data

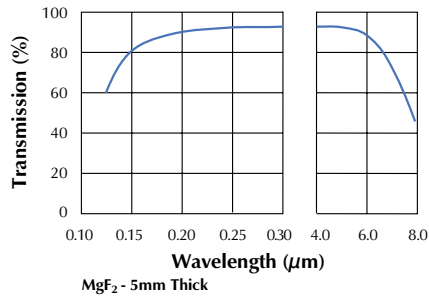
AR coatings on Fused Silica
193nm > 2 J/cm², 20ns, 20Hz
266nm, 355nm > 5 J/cm², 10ns, 10Hz

1064nm, 20ns, 20Hz data

| | |
|-----------------------------|-----------------------|
| AR coatings on Fused Silica | >20 J/cm ² |
| AR coatings on BK7 | >10 J/cm ² |
| AR coatings on SF11 | >4 J/cm ² |
| Optical Cement | >2 J/cm ² |
| HR coatings | >10 J/cm ² |

For higher damage thresholds call CVI to optimize the various material parameters and provide certification. CVI is a leader in damage resistant coatings for excimer and other high energy lasers.

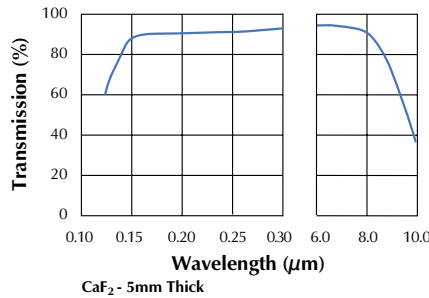




MgF₂

MgF₂ is a tetragonal positive birefringent crystal grown using the vacuum Stockbarger technique. MgF₂ is a rugged material resistant to chemical etching, mechanical, and thermal shock. High vacuum UV transmission and resistance to laser damage make MgF₂ a popular choice for VUV and excimer laser windows, polarizers, and lenses.

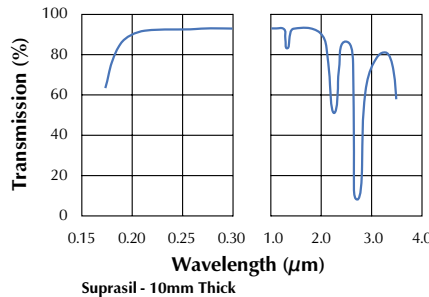
- **Thermal expansion coefficients:**
 $dn_o/dT: 2.3 \times 10^{-6}/^{\circ}C$
 $dn_e/dT: 1.7 \times 10^{-6}/^{\circ}C$
- **Hardness (Knoop): 415**
- **Density: 3.177 g/cm³**



CaF₂

CaF₂ is a cubic single crystal grown using the vacuum Stockbarger technique. Care must be used when thermally cycling CaF₂. Common CaF₂ uses include vacuum ultraviolet components such as excimer laser windows, lenses, and prisms. Contact CVI for additional information regarding Deep UV applications.

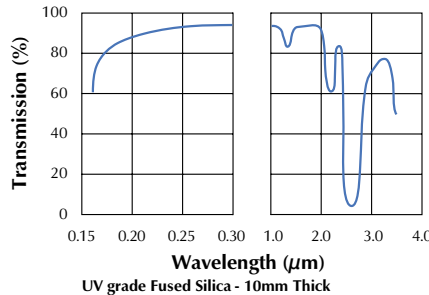
- **Thermal expansion coefficient: $18.85 \times 10^{-6}/^{\circ}C$ (20°C to 60°C)**
- **Hardness (Knoop): 160**
- **Density: 3.18 g/cm³**



Suprasil 1

Suprasil 1 is a type of fused silica with high chemical purity and excellent homogeneity in all axes. With a metallic content less than 8 ppm, Suprasil 1 has superior UV transmission and minimal fluorescence. Suprasil 1 is primarily used for low fluorescence UV windows, lenses, and prisms where multiple axis homogeneity is required.

- **Typical index homogeneity: $\Delta n < 8 \times 10^{-6}$**
- **Thermal expansion coefficient: $0.58 \times 10^{-6}/^{\circ}C$ (0°C to 200°C)**
- **Density: 2.201 g/cm³**

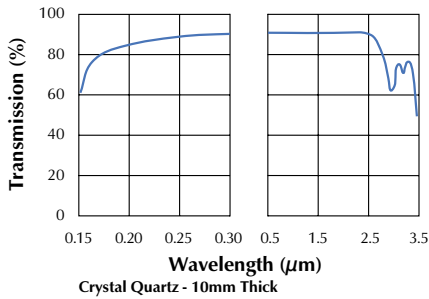


UV grade Fused Silica

UV grade Fused Silica is an amorphous form of silicon dioxide made by flame hydrolysis of silicon tetrachloride. Properties include high UV transmission, low thermal expansion coefficient, and high laser damage threshold. Used for UV windows, lenses, prisms, and mirror substrates.

- **Typical homogeneity: $\Delta n < 3 \times 10^{-6}$**
- **Thermal expansion coefficient: $0.57 \times 10^{-6}/^{\circ}C$ (0°C to 200°C)**
- **Hardness (Knoop): 500**
- **Density: 2.202 g/cm³**

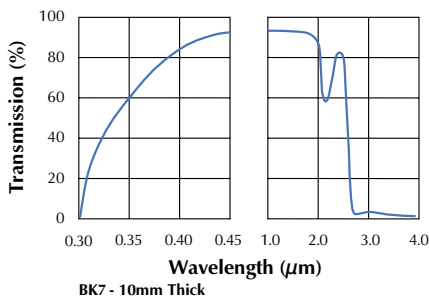
continued



Crystal Quartz

Crystal quartz is a positive uniaxial birefringent single crystal grown using a hydrothermal process. CVI's crystal quartz is selected to minimize inclusions and refractive index variation. Crystal quartz is most commonly used for high damage threshold waveplates and solarization resistant Brewster windows for argon lasers.

- **Thermal expansion coefficients:**
 $7.1 \times 10^{-6}/^{\circ}\text{C}$ parallel to [0001]
 $13.2 \times 10^{-6}/^{\circ}\text{C}$ perpendicular to [0001]
- **Density:** 2.649 g/cm^3

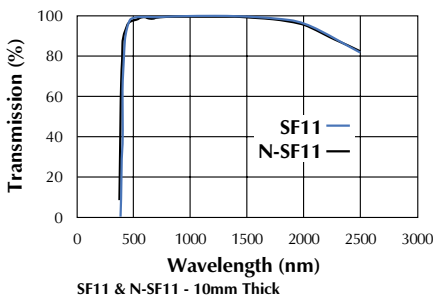


BK7

BK7 is a borosilicate crown optical glass with high homogeneity and low bubble content. This general purpose material is widely used in visible and NIR windows, lenses, and prisms.

- **Typical homogeneity:** $\Delta n < 1 \times 10^{-5}$
- **Thermal expansion coefficient:** $8.3 \times 10^{-6}/^{\circ}\text{C}$ (30°C to 300°C)
- **Hardness (Knoop):** 610
- **Density:** 2.51 g/cm^3

For up-to-date information on materials compliance with the European Union RoHS ► www.cvilaser.com



SF11 and N-SF11

SF11 and its lead-free equivalent (N-SF11) are high refractive index materials used to provide more optical power with less curvature. Used in achromats and other multi-element lenses to correct for chromatic aberrations, it exhibits lower LDT than BK7 or fused silica. CVI maintains inventory of both SF11 and N-SF11, please specify when ordering.

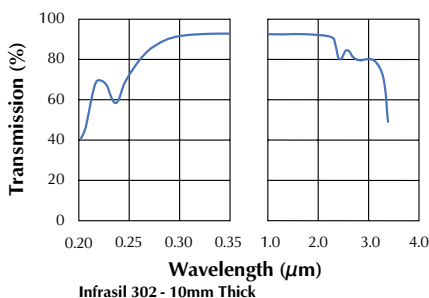
SF11

- **Thermal expansion coefficient:**
 $6.8 \times 10^{-6}/^{\circ}\text{C}$ (20°C to 300°C)
- **Hardness (Knoop):** 450
- **Density:** 4.74 g/cm^3

N-SF11

- **Thermal expansion coefficient:**
 $-1.4 \times 10^{-6}/^{\circ}\text{C}$ (20°C to 40°C)
- **Hardness (Knoop):** 615
- **Density:** 3.22 g/cm^3

For up-to-date information on materials compliance with the European Union RoHS ► www.cvilaser.com

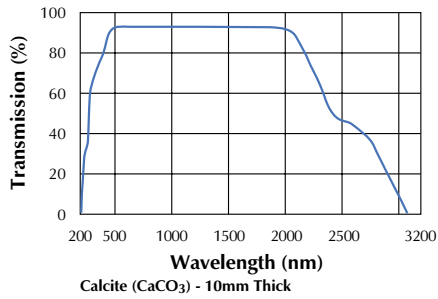


Infrasil 302

Infrasil 302 is a low OH content fused quartz. Fused quartz is produced by electrically fusing high quality quartz crystal. Infrasil 302 is used for applications where minimum OH absorption is required, including NIR high energy laser windows and lenses.

- **Typical homogeneity:** $\Delta n < 3 \times 10^{-6}$
- **OH content:** < 8 ppm
- **Thermal expansion coefficient:** $0.58 \times 10^{-6}/^{\circ}\text{C}$ (0°C to 200°C)
- **Density:** 2.203 g/cm^3

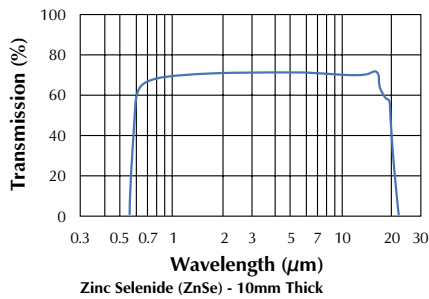
continued



Calcite (CaCO₃)

Birefringent crystal with wide spectral transmission. Most commonly used in visible and NIR polarizers: Glan Taylor, Glan Thompson and Glan laser. This soft material scratches easily. Take care in handling these polarizers.

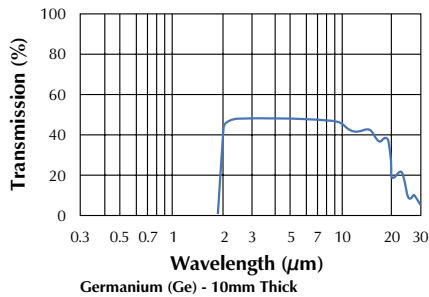
- **Thermal Expansion Coefficient:**
 $\alpha_a = 24.39 \times 10^{-6}/^{\circ}\text{C}$
 $\alpha_c = 5.68 \times 10^{-6}/^{\circ}\text{C}$
- **Hardness (Moh): 3**
- **Density: 2.71 g/cm³**



ZnSe

Zinc Selenide is well suited for windows, lenses and partial reflectors in the IR region due to its low absorption at these wavelengths and visible wavelength transmission.

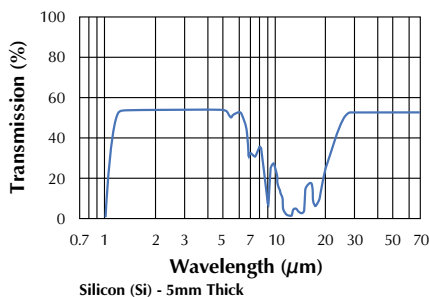
- **Refractive Index of 2.40 at 10.6μm and 2.60 at 632.8nm**
- **Transmission Region from 0.5 to 20μm**
- **Typical Bulk absorptivity (cm⁻¹ at 10.6μm) is 0.0005**
- **Thermal Expansion Coefficient:**
 $10^{-6}/^{\circ}\text{C}: 7.6$
 $\Delta n/\Delta T (10^{-6}/^{\circ}\text{C}): 64$
- **Hardness (Knoop): 100**
- **Density: 5.27 g/cm³**



Ge

Germanium is commonly used in imaging systems working in the 2 to 12μm wavelength region. Ideal substrate for lenses, windows and mirrors in low power CW and CO₂ laser systems.

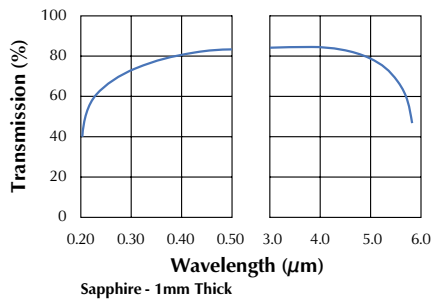
- **Refractive Index of 4.00 at 10.6μm**
- **Transmission Region from 2 to 23μm**
- **Typical Bulk absorptivity (cm⁻¹ at 10.6μm) is 0.035**
- **Thermal Expansion Coefficient:**
 $10^{-6}/^{\circ}\text{C}: 5.7$
 $\Delta n/\Delta T (10^{-6}/^{\circ}\text{C}): 277$
- **Hardness (Knoop): 692**
- **Density: 5.323 g/cm³**



Si

Silicon is an economical and lightweight material for use in IR applications.

- **Refractive Index of 3.42 at 6.0μm**
- **Transmission Region from 1.5 to 7μm**
- **Typical Bulk absorptivity (cm⁻¹ at 10.6μm) is 0.04 at 6.0μm**
- **Thermal Expansion Coefficient:**
 $10^{-6}/^{\circ}\text{C}: 4.15$
 $\Delta n/\Delta T (10^{-6}/^{\circ}\text{C}): 160$
- **Hardness (Knoop): 820**
- **Density: 2.33 g/cm³**



Sapphire

Sapphire is a synthetic hexagonal crystal form of aluminum oxide. Sapphire exhibits high mechanical strength, chemical resistance, and thermal stability. Unless otherwise specified, CVI supplies random axis orientation sapphires. Contact CVI for (0001) axis orientation.

- **Thermal expansion coefficient:** $8.4 \times 10^{-6}/^{\circ}\text{C}$ (20°C to 500°C)
- **Hardness (Knoop):** 1370
- **Density:** 3.97 g/cm³

Corning HPFS™ for Deep Ultraviolet Applications

HPFSTM, High Purity Fused Silica, Corning Code 7980, is a high purity synthetic amorphous silicon dioxide glass which combines a very low thermal expansion coefficient, excellent optical qualities, and exceptional transmission properties for ultraviolet applications. It is available in a number of grades for different applications.

Quality Grade Selection Chart

| Inclusion Class No. | Total Inclusion Cross-Section | Maximum Inclusion Cross-Section |
|---------------------|-------------------------------|---------------------------------|
| 0 | 0.00-0.03mm ² | 0.10mm (0.004") |

Notes:

- 1.Total Inclusion Cross-Section: Defines the sum of the cross-section in mm² of inclusions per 100cm³ of glass. Inclusions with a cross-section equal to or less than 0.10mm diameter are disregarded.
- 2.Maximum Inclusion Cross-Section: Refers to the diameter of the largest single inclusion in any single 100cm³ of glass.

Birefringence

| | |
|----------|--------------------------------|
| ≤ 2nm/cm | Lower specifications available |
|----------|--------------------------------|

248nm Induced Absorption

| Fluence (mJ/cm ²) | Number of Pulses (x 10 ⁶) | 248nm Induced Absorbance/cm |
|-------------------------------|---------------------------------------|-----------------------------|
| 250 | 5 | No Change |
| 400 | 1 | No Change |

Exposure Conditions: 400Hz, 16nsec pulse duration

Internal Transmittance

| |
|------------------------------|
| Ti = 99.8 ± 0.1%/cm at 248nm |
| Ti = 99.0 ± 0.2%/cm at 193nm |

Note:

Normalized to a 10mm thickness, surface reflection losses excluded.

Malitson's Dispersion Equation

$$n^2 - 1 = \frac{0.6961663\lambda^2}{\lambda^2 - (0.0684043)^2} + \frac{0.4079426\lambda^2}{\lambda^2 - (0.1162414)^2} + \frac{0.8974794\lambda^2}{\lambda^2 - (9.896161)^2}$$

Malitson I.H. Journal of the Optical Society of America: 1965 (λ=microns)

Index Homogeneity Grade

| Grade AA | Grade A |
|--------------------------|------------------------|
| ≤ 0.5 x 10 ⁻⁸ | ≤ 1 x 10 ⁻⁸ |

Notes:

1. Index Homogeneity: The maximum index variation (relative) measured over the clear aperture of the blank.
2. The minimum thickness for index homogeneity verification is 20.3mm (0.800"). For sizes less than 20.3mm thickness, the parent piece is certified.
3. Index homogeneity is certified using an interferometer at 632.8nm. The numerical homogeneity is reported as the average through the thickness.

Striae

| |
|--|
| MIL-G-174B: Class 1, Grade A (through thickness) |
|--|

193nm Induced Absorption

| Number of Pulses (x 10 ⁶) | 193nm Transmittance %/cm ±0.05 | 193nm Induced Absorbance/cm |
|---------------------------------------|--------------------------------|-----------------------------|
| 0 | 99.26 | 0.0 |
| 351 | 98.67 | 0.0026 ± 0.004 |
| 859 | 98.64 | 0.0027 ± 0.004 |

Exposure Conditions: 300Hz, 16nsec pulse duration, fluence 0.56mJ/cm²/pulse, 120mm pathlength

Refractive Index

| | |
|---------|------------------|
| 248nm | 1.508551 ± 25ppm |
| 193nm | 1.560769 ± 25ppm |
| 632.8nm | 1.457018 |

(calculated per Malitson)

continued

248nm and 193nm Densification Results

$\Delta\rho/\rho$ is defined as the unconstrained densification of the glass¹
[193nm: $\Delta\rho/\rho$ (ppm) = $a \times (NI)^b$ (N=Pulses, I=Fluence where $a= 91.00 \times 10^{-6}$, $b=0.53$)]
[248nm: $\Delta\rho/\rho$ (ppm) = $a \times (NI)^b$ (N=Pulses, I=Fluence where $a= 7.00 \times 10^{-6}$, $b=0.53$)]

| Wavelength (nm) | Number of Pulses (x 10 ⁶) | Dose ³ (NI2 x 10 ⁶) | $\Delta\rho/\rho$ (ppm) (Measured) ⁴ | $\Delta\rho/\rho$ (ppm) (Predicted) |
|--------------------|---|---|--|--|
| 193 | 32.0 | 5.73 ² | 0.39 | 0.447 |
| 193 | 532.0 | 157.00 | 2.38 | 2.580 |
| 193 | 662.1 | 207.60 | 2.71 | 2.990 |
| 248 | 0.5 | 7,565.00 | 1.06 | 1.231 |
| 248 | 6.0 | 90,774.00 | 4.40 | 4.481 |

- 1 The unconstrained densification of the glass is that which would occur under conditions of uniform illumination of a sample. The optical path difference, OPD, for a specific sample geometry and illumination profile can be derived from $\Delta\rho/\rho$ using elastic analysis.
- 2 The fluence was 0.42 mJ/cm²/pulse. All other samples were tested at 0.56 mJ/cm²/pulse.
- 3 Exposure conditions 248nm: 400Hz, 16nsec pulse duration, fluence 123 mJ/cm²/pulse, 120mm pathlength.
Exposure conditions 193nm: 300Hz, 16nsec pulse duration, fluence 0.56 mJ/cm²/pulse, 120mm pathlength.
- 4 Measurements are made through the 12 cm path length on an interferometer at 632.8nm. Measurement error \pm 0.04.

References:

(a) 193 nm Excimer Laser Induced Densification of Fused Silica, D.C. Allan, C. Smith, N.F. Borrelli, T.P. Seward III. Corning Incorporated, Corning N.Y. 14831. Optics Letters 1960, 1996. (b) Densification of Fused Silica Under 193 nm Excitation, N.F. Borrelli, C. Smith, D.C. Allan, T.P. Seward III. Corning Incorporated, Corning N.Y. 14831. Accepted for publication JOSA, B, July 1997.

Suprasil® for Excimer Laser Applications

Not all fused silica materials are alike.

This is especially true for deep UV applications, where the purity and chemical make-up of the glass may affect performance. All fused silica made today is subject to laser damage (in the form of absorption and/or compaction) when exposed to high intensity deep UV radiation from excimer sources. For a given fused silica, the amount of UV damage, measured by either changes in absorption, refractive index, or fluorescence, depends on the laser parameters (i.e. wavelength, energy density, number of pulses, and pulse width).

Start with well defined, consistent materials.

Heraeus Quarzglas GmbH, in Hanau, Germany, has done some of the most extensive UV laser research on fused silica materials in the world (see references #3 & #5). They have learned how to properly measure UV absorption (which is often a transient or time dependent characteristic).

Heraeus first learned how to measure, characterize, and model different types of fused silica, then they developed process improvements to optimize their materials. Today, Heraeus Suprasil 1 or 2 and Suprasil 312 or 311 are the most widely used materials for deep UV applications.

Because Heraeus' unique manufacturing processes are consistent and repeatable, they produce extremely homogeneous material that has become the material of choice, worldwide, for DUV microlithography applications as well as broadly applied excimer laser applications.

But what conditions cause damage?

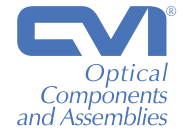
For high light intensities (created by excimer lasers), the interaction between UV photons and the optical material must be taken into account. UV photons may generate defect centers, resulting in an aging of components (UV radiation damage). Induced absorption, induced refractive index change (or "compaction"), and induced fluorescence are of significant importance. A broad statement cannot be made covering all applications. Laser damage is highly dependent on the application.

The damage behaviors of two fused silica types, Suprasil® 2 and Suprasil® 312, differ dramatically. One can learn more about fused silica and DUV laser interaction from the papers listed below.

References:

1. D. Griscom, Optical Properties and Structure of Defects in Silica Glass (J. Ceram. Soc. Jap., 1991), p. 99, 899-916.
2. D.J. Kraijnovich, I.K. Pour, A.C. Tam, W.P. Leung, and M.V. Kulkarni, 248nm Lens Materials: Performance and Durability Issues in an Industrial Environment (SPIE, 1848, 1993), p. 544.
3. N. Leclerc, Ch. Pfeleiderer, H. Hitzler, J. Wolfrum, K.O. Greulich, St. Thomas, H. Fabian, R. Takke, and W. Englisch, Transient 210nm Absorption in Fused Silica Induced by High-Power UV Laser Irradiation (Opt. Lett., 1991), p. 16(12), 940-942.
4. B. Scruggs and K.J. Gleason, The Role of Proton Nuclear Magnetic Resonance Spin-Lattice Relaxation Centers in the Strong Absorption Transition at 210nm in Fused Silica (J. Appl. Phys., 1994), p. 76(5), 3063-3067.
5. St. Thomas, W. Englisch, and R. Takke, Effect of Excimer Laser Radiation on the Optical Properties of Synthetic Fused Silica (Glass Sci. Techn., 1994), p. 67C, 19.
6. St. Thomas and B. Kühn, KrF Laser Induced Absorption in Synthetic Fused Silica (Heraeus Quarzglas GmbH, 1996).

Antireflection Coatings



Technical Notes

- **Largest selection of designs, 193nm-13.5μm**
- **User-specified wavelengths**
- **Optimal design is automatically provided on CVI partial reflectors, beamsplitters, and dichroics**
- **Single layer, V-type, BBAR, and special designs**
- **R < 0.25%, 0°, at single wavelengths**
- **R < 0.5% avg, 0°, over wide ranges**
- **Coatings available optimized for 45° with high durability and damage threshold**

Antireflection (AR) coatings are required to reduce overall transmission loss, minimize stray light, and prevent back reflections. Stray light in the wrong place can swamp the desired signal, making a measurement impossible. Reflected laser beams can burn absorbing surfaces, form unwanted foci, and pose safety hazards, while back-reflected beams can destabilize laser oscillators. For these reasons, obtaining the proper AR coating can be a critical factor in system success. CVI offers over thirty years of experience in helping scientists and engineers choose the proper AR coating for optimum performance.

CVI can provide a standard or custom design to solve almost any AR coating requirement. V-type AR and Broadband AR designs are available from 193nm to 13.5μm. CVI antireflection coatings are the most durable and damage resistant in the industry.

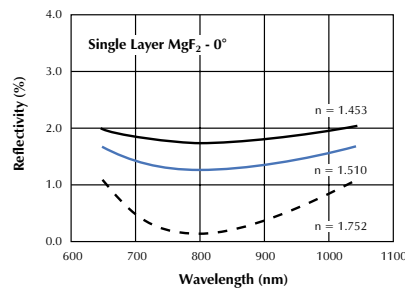
Antireflection coatings can be divided roughly into 4 categories: Single layer AR coatings, V-type AR coatings, BBAR coatings, and special purpose AR coatings.

1. Single Layer MgF₂ Coatings

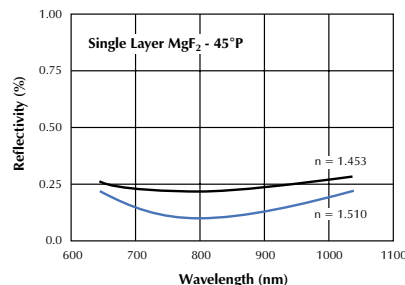
- **R < 0.25%, 0°, over wide ranges on sapphire, Nd:YAG, and high index glasses**
- **R < 0.25%, 45°P on crown glass and fused silica**

The CVI single layer MgF₂ AR coating is an excellent choice for use on high index materials at normal incidence. Such materials include sapphire, Nd:YAG, ruby, and SF10 and SF11 glasses. On crown glass or fused silica, the MgF₂ index of about 1.38 is too high to provide a good impedance match at the air-glass interface, yielding a residual reflectivity of about 1.3%. For these materials, V-type and BBAR coatings with reflectivities from 0.25% to 0.5% are the best choice at normal incidence. Shown below are graphs of the performance of MgF₂ on different materials at normal incidence, and at 45°P on glass and fused silica.

Single Layer MgF₂ AR Designs for 0°



Single Layer MgF₂ AR Designs for 45°



2. V-type Antireflection Coatings

- **R < 0.25% at design wavelength, 0°**
- **R < 0.75% at design wavelength, 45° unpolarized**
- **Included on the second surface of all CVI single line beam splitters and partial reflectors**
- **All laser wavelengths available**
- **Highest durability and damage threshold**

CVI's V-type AR coatings are the best choice for a single laser wavelength or multiple, closely-spaced wavelengths. Examples are the principle argon laser lines at 488nm and 515nm, the neodymium transitions in a variety of host materials at 1047-1064nm, and the individual excimer laser lines.

CVI will manufacture V-type AR coatings for wavelengths from 193nm to 10.6μm.

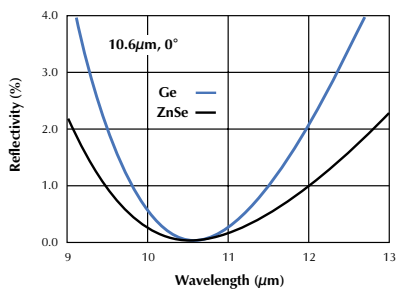
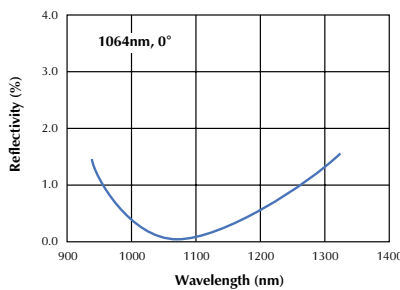
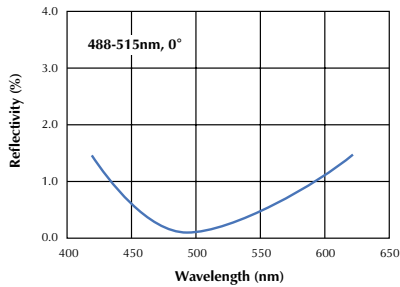
V-type AR coatings on Fused Silica, Crystal Quartz, Suprasil, and BK7 have a damage threshold of 15J/cm² at 1064nm, 20ns, 20Hz. Typical performance can often exceed 20J/cm².

Damage thresholds for AR coatings on SF11 and similar glasses are limited not by the coating, but by the bulk material properties. Our damage testing has shown a damage threshold for SF11 and similar glasses to be 4J/cm².

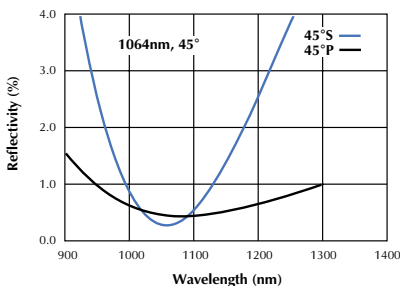
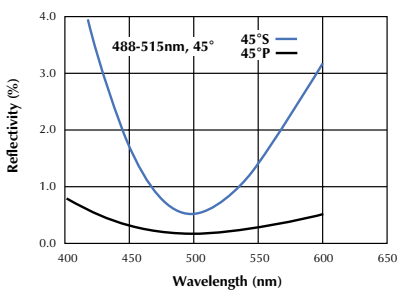
When ordering, be sure to specify the following:

- **Wavelength**
- **Substrate material**
- **Angle of incidence**
- **Polarization**
- **Fluence in J/cm²**

V-Type AR Designs for 0°



V-Type AR Designs for 45°

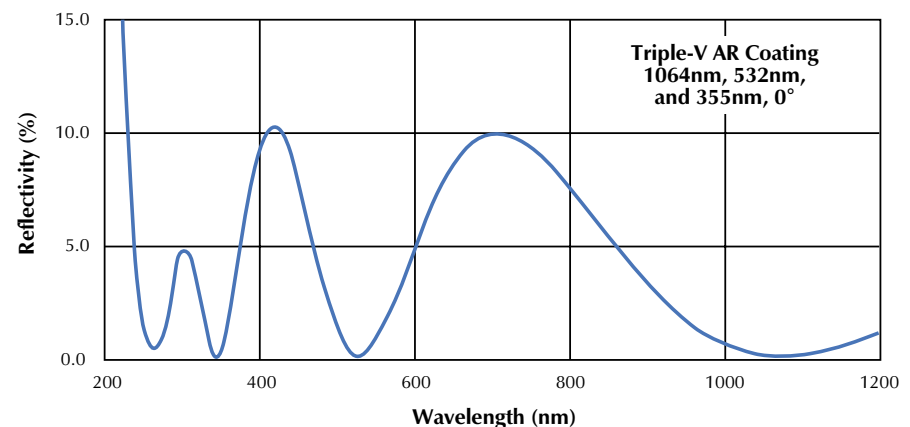
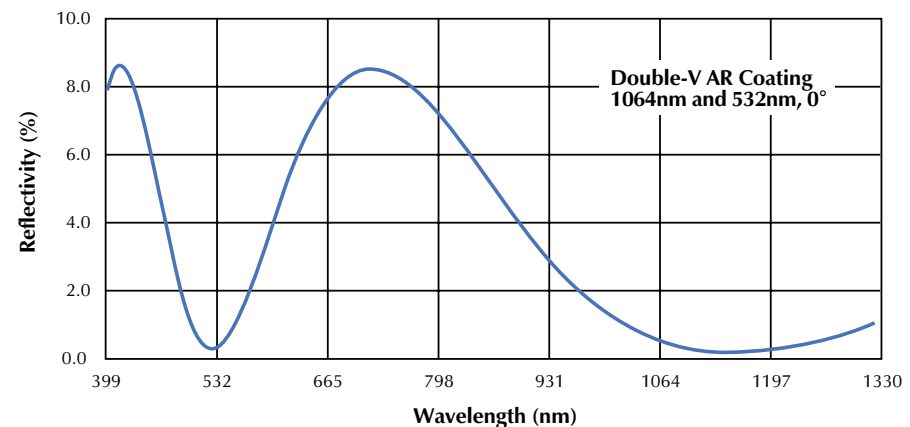


3. Double-V and Triple-V AR Coatings

- Available at Nd:YAG wavelengths
1064nm, 532nm, and 355nm
- Double-V:
R < 0.3% at 1064nm, 0°
R < 0.6% at 532nm, 0°
- Damage threshold for Double-V
5J/cm² at 532nm
10J/cm² at 1064nm
- Triple-V:
R < 0.3% at 1064nm, 0°
R < 0.6% at 532nm, 0°
R < 1.5% at 355nm, 0°

CVI offers Double-V and Triple-V multilayer AR coatings for use in Nd:YAG laser systems at normal incidence. Highly

damage resistant, electron beam deposited dielectrics are used exclusively as coating materials. As shown in the curves, the antireflection peaks at the harmonics are quite narrow. Also, due to the coating design and dispersion, they do not fall exactly at a wavelength ratio of 1 : 1/2 : 1/3. Consequently, the reflectivity specifications of these AR coatings are not as good as V coatings for any one wavelength. CVI offers these Double-V coatings on **W2** windows ► **10**, in all standard sizes. Contact CVI for the performance of 45° Double-V and Triple-V AR coatings or for other harmonic combinations.



continued

4. Broadband Antireflection Coatings

- **R < 0.5% average over very wide ranges at 0°**
- **R < 1.5% for 45°UNP**
- **R < 3.0% for 45°S**
- **R < 0.5% for 45°P**
- **Eleven standard designs covering UV to IR**
- **Custom wavelength bands available**

CVI offers broadband antireflection (BBAR) coatings optimized to your specifications over the entire range of 193nm to 13.5μm. A selection chart is provided on this page showing CVI standard coating ranges.

If your tuning range or wavelength band falls within the bold lines on the selection chart, CVI can manufacture a special BBAR coating for you.

BBAR coatings are often designed by inserting a half wave thick "absentee" layer between the layers of a V-type AR coating. This dramatically broadens the range of effectiveness of the AR coating. CVI guarantees that the average reflectance of most BBAR coatings will be less than 0.5% at normal incidence.

For the lowest possible reflectance at a single wavelength, the V-type antireflection coating is the best choice. In many applications, however, the BBAR coating will work extremely well, with the added advantage of a wider range of use.

Contact CVI for details regarding specialty BBAR designs including the Super BBAR 400-1100nm and the visible/1064nm combination coating.

Typical damage threshold is 10J/cm² at 1064nm.

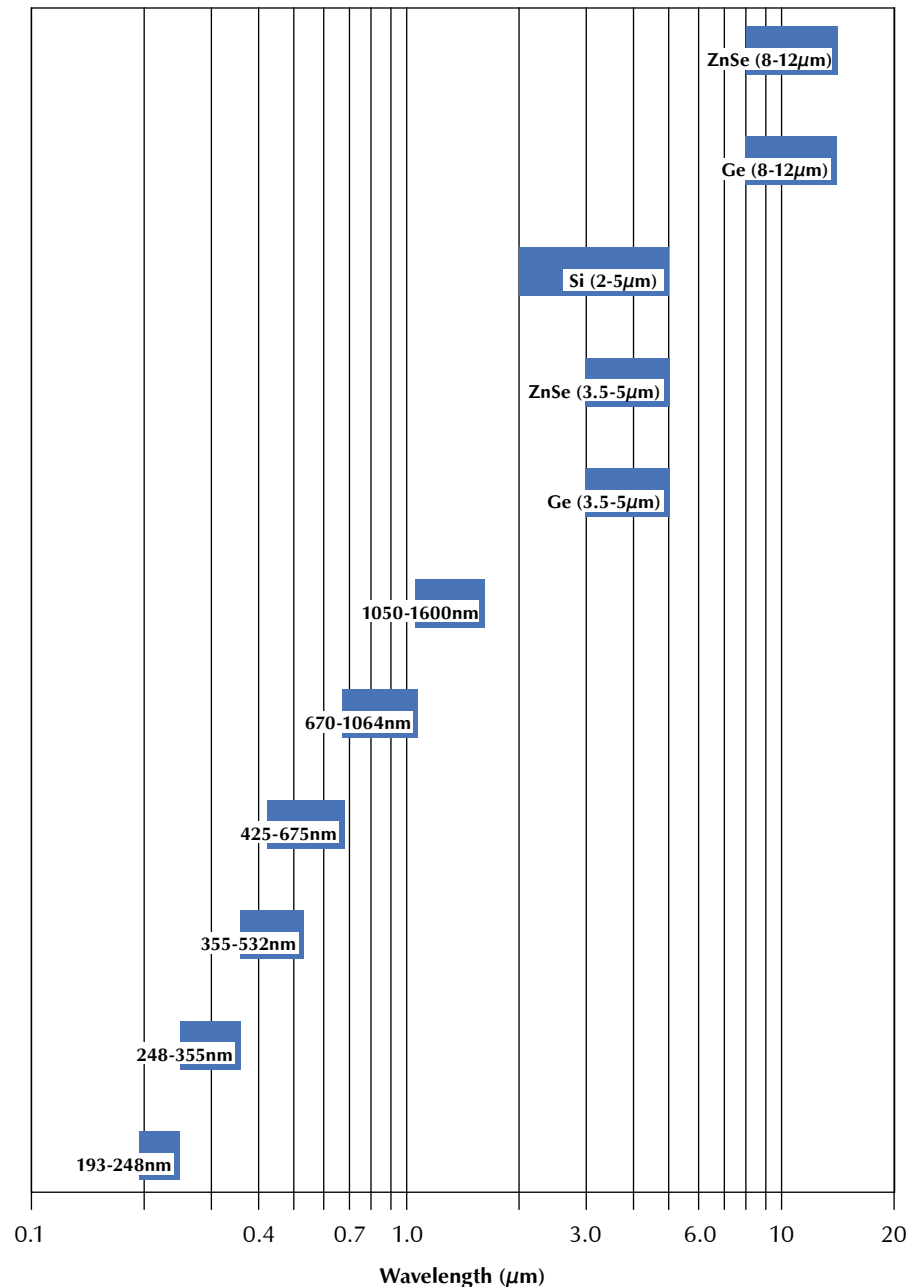
BBAR Selector Data

UV, VIS, NIR, and IR Regions

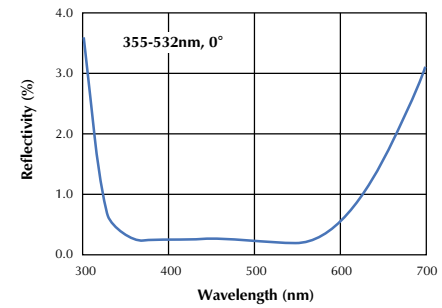
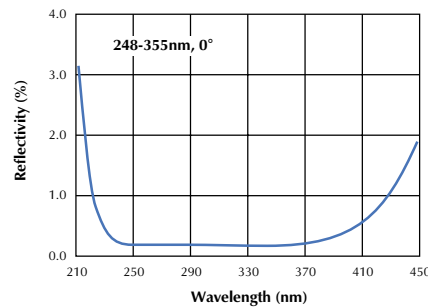
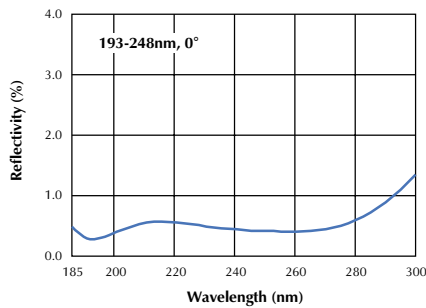
CVI offers six overlapping designs covering the entire range from 193nm to 1600nm. This includes very broad coverage of the entire Ti:Sapphire region through the near IR. In addition, the mid to far IR regions are available from standard CVI BBAR coatings

shown. Typical performance curves are shown in the graphs on the following page. Many research and instrumentation applications can be covered by a single judicious choice of region. If your application cannot be covered by a standard design, CVI can provide a special BBAR coating design.

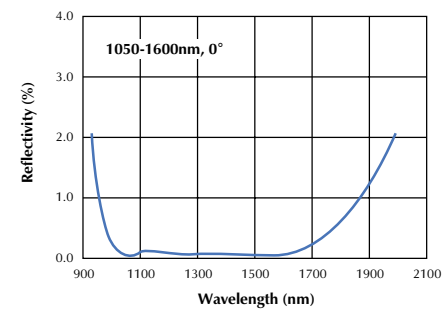
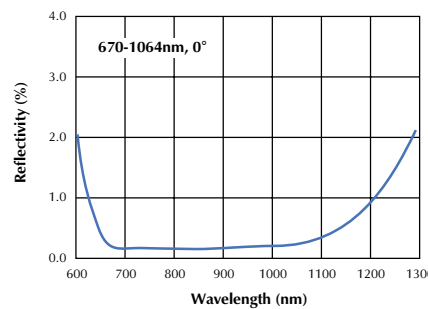
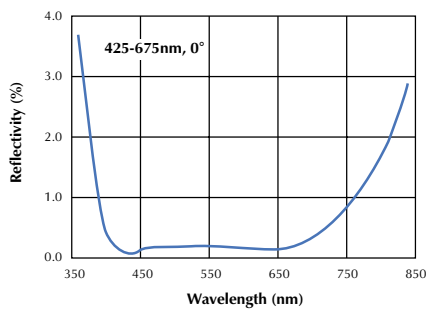
CVI Standard Broadband Antireflection Coatings



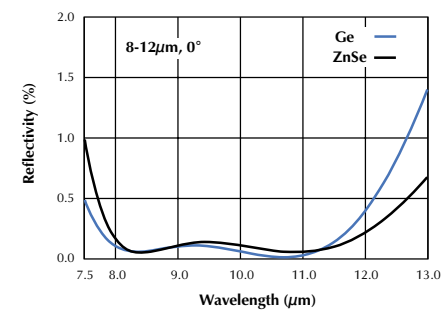
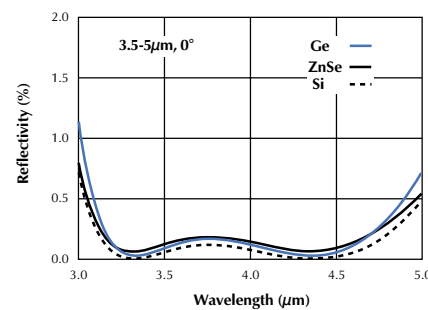
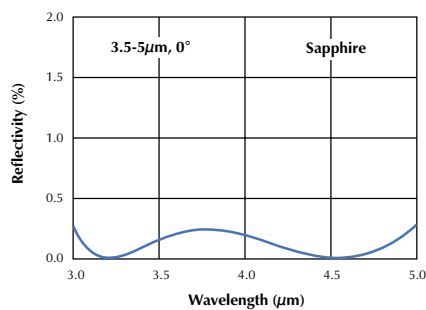
UV region Broadband AR coating designs for 0°



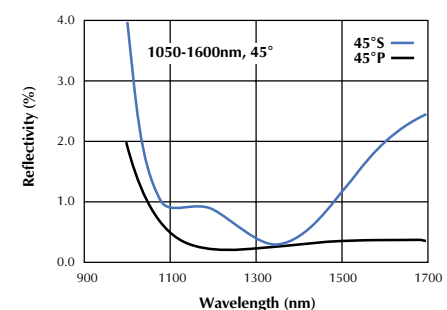
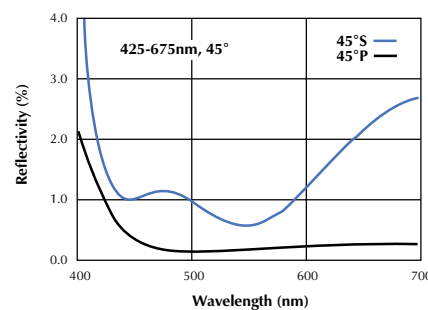
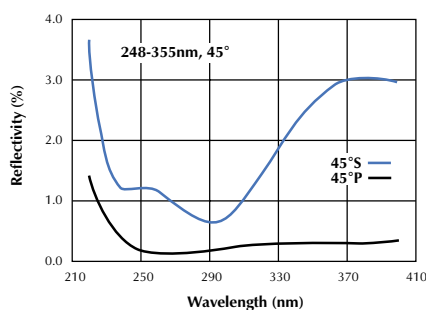
VIS and near IR region Broadband AR coating designs for 0°



IR region Broadband AR coating designs for 0°



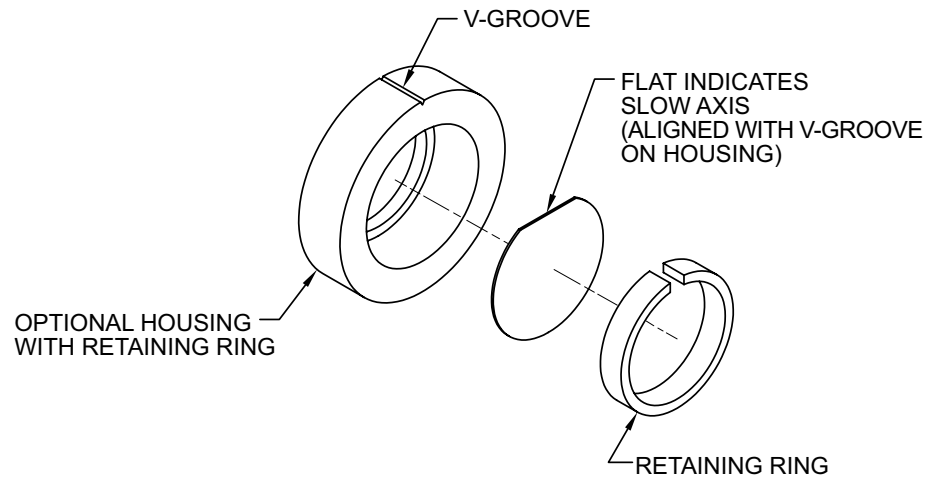
Typical Broadband AR coating designs for 45°S and 45°P



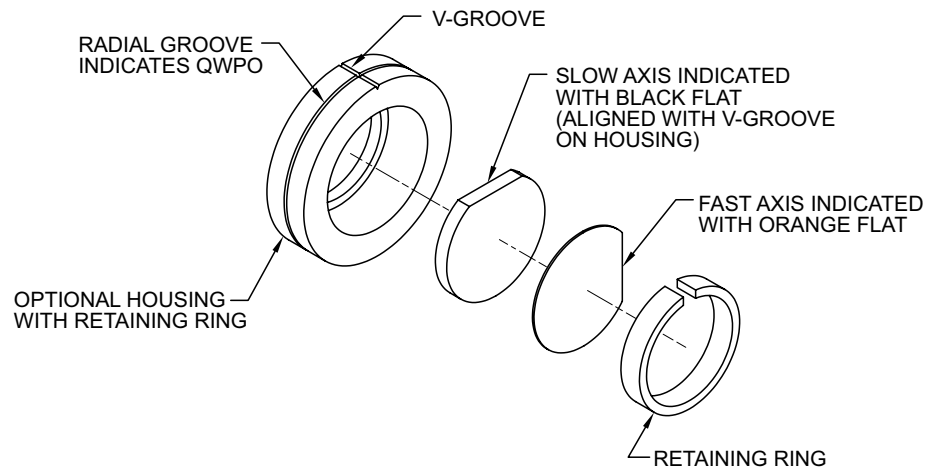
Waveplate Optical Axis Markings

Technical Notes

QWPM Waveplate Assembly



QWPO Waveplate Assembly



QWPO Air-Spaced Waveplate Assembly

